Adaptive Wind Feedforward Control of an Unmanned Surface Vehicle for Station Keeping

Huajin Qu and Karl D. von Ellenrieder, Member, IEEE
Department of Ocean & Mechanical Engineering
Florida Atlantic University, 101 N. Beach Rd. Dania Beach, FL USA
Email: hqu@fau.edu

Abstract— **Unmanned Surface Vehicles (USVs) have widespread commercial, scientific and military applications. In some of these applications station keeping is essential. Since USVs have a bigger surface/ weight ration than large commercial ships, they are more sensitive to wind disturbances, especially during station keeping. The modeling, identification and control of a 4.9 meter long, 180 kilogram wave adaptive modular vehicle (WAM-V) USV are presented in this paper. The propulsion system of the USV is custom designed with two azimuthing thrusters, making the USV fully actuated. System identification tests were conducted to get the precise model of the USV. A sliding mode controller was first applied to the USV and a wind feedforward controller was designed to aid the nonlinear feedback control to mitigate wind disturbance. For the feedforward controller design, a wind model was formulated that uses the apparent wind speed and direction collected from a high accuracy anemometer. A model based adaptive mechanism was developed to tune the feedforward control gains for the best performance. Station keeping field tests were conducted at a location with an average wind speed of 9 knots. The results show that with the tuned feedforward controller, the USV can hold its position and heading better over extended periods of time than a single feedback controller.**

Keywords*— *Wind Feedforward Control, Unmanned Surface Vehicles, Station Keeping, automatic tuning

I. INTRODUCTION

Unmanned Surface Vehicles (USVs) are widely used for commercial, military, and scientific applications, such as environmental monitoring, oil and gas exploration, oceanographic data collection and recovery of underwater vehicles [1], [2]. Maintaining a fixed position and heading are required most of the time. For example, one potential application of the USVs is bridge inspection. The performance of the task will be heavily affected if wind, wave or current disturbances cause the vehicle to drift away. Therefore, station keeping is a key element for USVs to conduct their tasks.

Station keeping is an important application for marine vehicles. For large commercial ships (with an overall length of 200-400 m, and in the 150,000-500,000 DWT range) that have direct control over sway direction, station keeping allows them to avoid luxury of anchoring or mooring. The vehicle utilized in this paper is a small size USV that has an overall length of 4.9 m, weight of 180 kilograms. Compared to large commercial ships, it doesn't possess control in its sway axis, so the station keeping task is more challenging. However, the propulsion system of the USV is custom designed so that it has redundant control inputs and is fully actuated. More details of the USV and the propulsion system are in section II.

The study of station keeping control of USVs has increasingly grown. The majority of the efforts focused on linear and nonlinear feedback control methods. For example, [3] presented the use of acceleration feedback in dynamic positioning. [4] described an asymptotic manner using accurate visual position feedback for station keeping. In [5], discontinuous stabilization control with backstepping approach was designed. And in paper [6] a method of combining trajectory planning, tracking control based on nonlinear sliding mode control was presented. The paper [7] gave a thorough tutorial of nonlinear backstepping control theory with examples. A sliding mode controller that utilized in previous study [8], [9] on the station keeping of the USV was adopted here.

For large ships, feedback controllers, especially the integral part can attenuate slow varying environmental changes, and wind gust is generally considered unnecessary for the control system because of the slower dynamics [1]. However, for the small size of USVs, rapid change of wind speed and direction can have a severe effect on them. In this situation, feedforward feature is advantageous because it can reduce the burden of feedback controllers, and receive prompt response in rapid changing environment. In conjunction with nonlinear sliding mode feedback controller, the wind feedforward controller enables the USV to achieve more accuracy station keeping than is possible with feedback controller alone. While the feedback controller is designed to enhance the robustness of system for unknown disturbances, the feedforward controller can serve to foresee the disturbance before it acting on the system. However, compared to feedback control theory, feedforward has still not been widely explored. In [10], a weighted controller that uses wind feed-forward to complement a Line-of-Sight guidance controller on an under-actuated surface vehicle was designed and tested both in simulation and experiments. Most wind models, capable to estimate wind forces and moments acting on small marine vessels, are based on large vessels and floating objects in the ocean, such as oil tanks, and commercial ships [11], [12], [13], [14], [15]. These models need to be scaled for small size vehicles.

.

978-0-933957-43-5 ©2015 MTS

In order to get the best performance of wind feedforward controller, a feedforward tuning method was desired. Feedforward tuning is widely explored in the literature and is often used in industrial applications. In [18], three methods of feedforward controller tuning, namely Iterative Learning Control (ILC), Iterative Feedback Control (IFC), and Adaptive Feedforward Control (AFC) were presented. The ILC method updates the control law based on the information obtained from previous experiments. The IFC is an iterative method that tunes the control parameters to minimize a cost function. In AFC, uncertain parameters are estimated in real time to form the control input. In paper [19] adaptive feedforward control algorithms were given and experimental evaluation shown excellent error reduction. Two feedforward control methods were discussed in [20], namely infinite impulse response filter that designed off-line, and finite impulse response filter that adapted on-line using filtered-x LMS algorithm. In [21], an extreme learning control framework using a feedforward network was proposed, and output weights of the feedforward were updated by adaptive projection-based laws derived using a Lyapunov approach.

II. The USV 16

The USV utilized for this research is a Wave Adaptive Modular-Vehicle (WAM-V) USV16 (Fig. 1). The lengths, mass and overall beam are 4.88 m, 180 kg and 2.44 m respectively. The main characteristics are given in TABLE I.

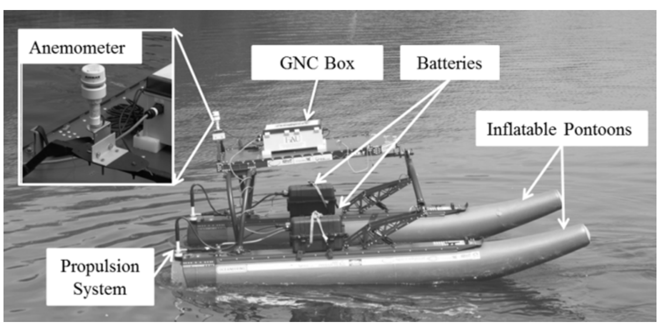

Fig. 1: The WAM-V USV16 during on-water station-keeping tests in the Intracoastal Waterway

TABLE I
PRINCIPLE CHARACTERISTICS OF THE WAM-V USV16. THE LOCATION OF THE "KEEL" IS TAKEN AS THE BOTTOM OF THE PONTOONS. W.R.T. IS AN ACRONYM FOR THE PHRASE "WITH RESPECT TO".

Parameter	Value
Length Overall (L)	4.88 [m]
Length on the Waterline (LWL)	3.20 [m]
Draft (aft and mid-length)(lightship)	0.30 and 0.23 [m]
Beam Overall (B)	2.44 [m]
Beam on the Waterline (BWL)	2.39 [m]
Depth (keel to pontoon skid top)	0.43 [m]
Area of the Waterplane (AWP)	1.6 [m^2]
Centerline-to-centerline Side Hull Separation (BCC)	1.83 [m]
Length to Beam Ratio (L/B)	2.0
Volumetric Displacement (∇) (lightship)	0.5 [m^3]
Mass	180 [kg]
Longitudinal Center of Gravity (LCG) w.r.t. aft plane of engine pods	1.30 [m]

A. Propulsion system

The propulsion system is custom designed and provides a peak thrust of 240N. This includes two 120 N electric thrusters, each powered by a 12V lead acid battery, and two 160 N, 15 cm stroke, linear actuators capable of rotating the thrusters through an azimuthal angle of $\pm 45^o$with respect to the vehicle's longitudinal direction, so that the USV is fully-actuated. The propulsion system and thrust directionality can be seen in Fig. 2and Fig. 3 respectively.

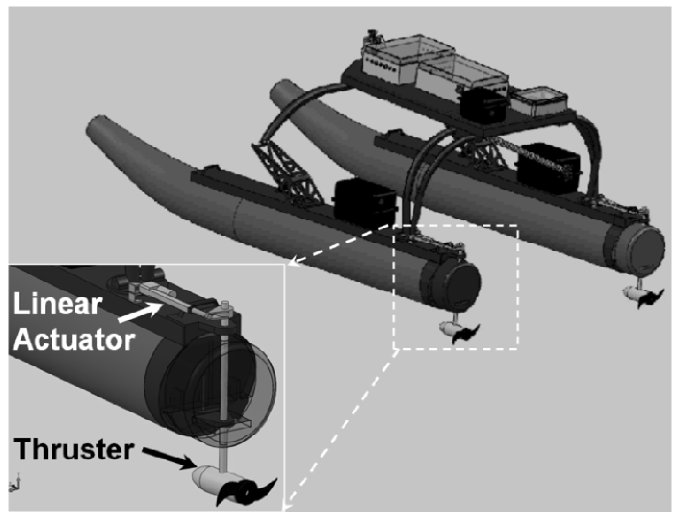

Fig. 2: WAM-V USV16 propulsion system

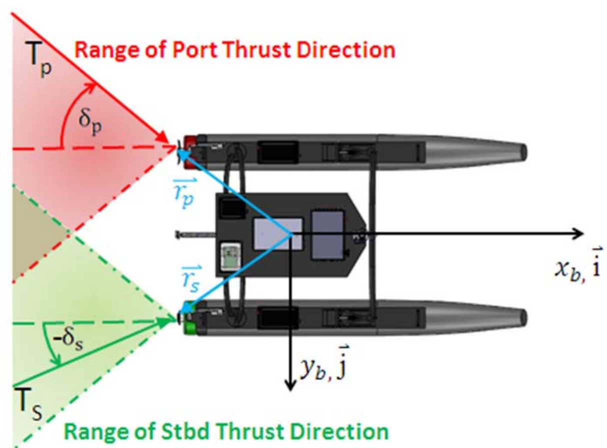

Fig. 3: Port and starboard thrust ranges directions. Both port and starboard can provide thrust at ±45° from hull centerlines.

B. Guidance, Navigation and Control (GNC) system

The GNC system of the USV includes IMU/GPS, digital compass, single-board computer, and RF transceiver, as shown in Fig. 1. The vehicle state information, namely position, heading, and velocity of the can be measured with high accuracy with IMU/GPS and compass. The real time state information will be relayed to a single board computer.

When the USV conducts its tasks, such as station keeping or trajectory tracking, it will be first engaged in manual remote control mode with RC controller to the desired initial location and then be switched to autonomous mode. Remote control can also serve to bring the USV back rapidly in emergency. A detailed description of the guidance, navigation and control (GNC) system implemented on the WAM-V USV16 was based on previous studies of WAM-V USV12 and USV 14, and can be found in [22], [23], [24].

C. Anemometer

An ultrasonic anemometer is used to measure the apparent wind speed and direction. The dynamic range of the sensor is 0-40 m/s with resolution of 0.1 m/s. Additional sensor specifications can be seen TABLE II. The wind speed and direction data collected with the sensor are filtered and passed to the feedforward controller. The anemometer is installed in an elevated position at the aft end of the payload tray to avoid the effects of wind blockage and interference from other structures (Fig. 1). Owing to the relatively small size of the USV, it is assumed that the wind speed and direction measured by a single point sensor is representative of the wind flowing past the entire vessel.

TABLE II
ANEMOMETER SPECIFICATIONS

Parameter	Value
Wind Speed Range	0 to 40 [m/s]
Wind Speed Resolution	0.1 [m/s]
Wind speed accuracy (no precipitation)	0.5[m/s]
Wind direction range	0-360[deg]
Wind direction resolution	0.1[deg]
Wind direction accuracy	2-8[deg]
Weight	300[grams]
Communication interface	RS232

III. EQUATION OF MOTION

It is convenient to define the body-fixed frame and earth-fixed frame when describing the motion of craft. The body-fixed frame is fixed to the vehicle and is a moving coordinate system. The linear and angular velocities of the craft as well as the forces and moment acting on the vehicle are described in the body frame. The earth-fixed reference, with axis point towards North, East and downwards normal to the earth surface, is called the North-East-Down (NED) coordinate system [25]. The position and orientation vector are described in this frame. These coordinate systems can be seen in Fig. 4. Throughout this paper, a three degree of freedom (DOF), namely surge, sway, and yaw model, are used to represent the motion of USV 16.

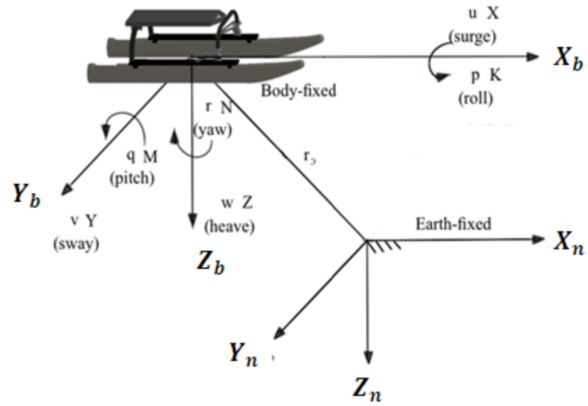

Fig. 4: Body-fixed (X_b, Y_b, Z_b) and earth-fixed (X_n, Y_n, Z_n) reference frame. . X, Y, and Z are the applied surge, sway and have forces, respectively. K, M, and N are the applied roll, pitch and yaw moments, respectively. u, v, and w are the surge, sway and heave speeds (respectively) in body fixed coordinates. Lastly, p, q and r are the roll rate, pitch rate and yaw rate, respectively.

The rigid-body dynamics is:

$$\dot{\boldsymbol{\eta}} = \boldsymbol{J}(\boldsymbol{\eta})v \tag{1}$$

The vector $\dot{\boldsymbol{\eta}}$ describes the vehicle's North ($\dot{x}$), East ($\dot{y}$) velocities and the angular velocity ($\dot{\psi}$) around the z axis in an inertial reference frame, $\boldsymbol{\eta} = [x, y, \psi]^T$ and the vector $\boldsymbol{v}$ contains the vehicle surge velocity (u), sway velocity (v) and yaw rate (r) in the body.

The transformation matrix between earth-fixed frame and body-fixed frame:

$$\boldsymbol{J}(\boldsymbol{\eta}) = \begin{bmatrix} \cos\psi & -\sin\psi & 0 \\ \sin\psi & \cos\psi & 0 \\ 0 & 0 & 1 \end{bmatrix}. \tag{2}$$

If we only consider wind as environmental disturbance, the equation of motion can be expressed as:

$$\boldsymbol{M}\dot{\boldsymbol{v}} + \boldsymbol{C}(\boldsymbol{v})\boldsymbol{v} + \boldsymbol{D}\boldsymbol{v} = \boldsymbol{\tau} + \boldsymbol{\tau}_{\boldsymbol{w}}, \tag{3}$$

$$\dot{\boldsymbol{\eta}} = [\dot{x}\ \dot{y}\ \dot{\psi}]^T, \tag{4}$$

$$\boldsymbol{v} = [u\ v\ r]^T. \tag{5}$$

Where $\boldsymbol{M}$ is an inertia tensor that contains both the rigid body mass matrix, and added mass matrix. $\boldsymbol{C}(\boldsymbol{v})$ is the Coriolis matrix, and can be removed from equation of motion without much loss of precision in station keeping for its low speeds. $\boldsymbol{D}(\boldsymbol{v})$ is the drag matrix and $\boldsymbol{\tau}$ is the vector of the forces and moment generated by vehicle's thrusters.

$$M = \begin{bmatrix} m - X_{\dot{u}} & 0 & 0 \\ 0 & m - Y_{\dot{v}} & 0 \\ 0 & 0 & I_z - N_{\dot{r}} \end{bmatrix}, \tag{6}$$

$$C(v) = \begin{bmatrix} 0 & 0 & -(m - Y_{\dot{v}})v \\ 0 & 0 & (m - X_{\dot{u}})u \\ (m - Y_{\dot{v}})v & -(m - X_{\dot{u}})u & 0 \end{bmatrix}, \tag{7}$$

$$D = \begin{bmatrix} X_u & 0 & 0 \\ 0 & Y_v & 0 \\ 0 & 0 & N_r \end{bmatrix}, \tag{8}$$

$$D_n = \begin{bmatrix} X_{u|u|}|u| & 0 & 0 \\ 0 & Y_{v|v|}|v| + Y_{v|r|}|r| & Y_{r|v|}|v| + Y_{r|r|}|r| \\ 0 & N_{v|v|}|v| + N_{v|r|}|r| & N_{r|v|}|v| + N_{r|r|}|r| \end{bmatrix}$$

$$\tau = \begin{bmatrix} T_x \\ T_y \\ M_z \end{bmatrix}. \tag{9}$$

T_x , T_y and M_z are the thrust in x_b and y_b direction, and resulting moment around the z_b axis. The USV generates the propulsion forces and turning moment with two azimuth thrusters, providing respectively Revolutions Per Minute (RPM) $n = [n_{p,} n_s]^T$, and thruster turning angles $\delta = [\delta_{p,} \delta_s]^T$ (Fig. 3). The subscript s and p stand for starboard and port sides respectively. We assume thrust has a linear relationship with RPM, so that $T = \frac{\delta}{\delta_{max}} \times 240\, N$, where $240\, N$ is the peak thrust. T_x , T_y and M_z can be calculated in (10)-(14). $\boldsymbol{\tau_w}$ denotes the forces and moments caused by wind.

$$T_x = (\boldsymbol{T_p} + \boldsymbol{T_s}) \cdot \boldsymbol{i} \tag{10}$$

$$T_y = (\boldsymbol{T_p} + \boldsymbol{T_s}) \cdot \boldsymbol{j}. \tag{11}$$

$$M_z = \boldsymbol{r_p} \times \boldsymbol{T_p} + \boldsymbol{r_s} \times \boldsymbol{T_s} \tag{12}$$

$$\boldsymbol{r_p} = -L\boldsymbol{i} - \frac{B}{2}\boldsymbol{j} \tag{13}$$

$$\boldsymbol{r_s} = -L\boldsymbol{i} + \frac{B}{2} \tag{14}$$

Where $\boldsymbol{r_p}$, $\boldsymbol{r_s}$ are vectors of port and starboard moment arms, and L is the distance between the center of gravity and the thruster, and B is overall beam (Fig. 3). For station keeping operation, nonlinear drag terms can be neglected.

A wind model was also designed for estimation of the wind loads in surge, sway and yaw direction. Several models can be found in the literature [26][27][28][29]. The one adopted here is based on [25].

For marine vehicles that have a forward speed, the dynamic pressure is:

$$q = \frac{1}{2}\rho_a V_{rw}^2, \tag{15}$$

Where $\rho_a = 1.2\, kg/m^3$ is the air density, and V_{rw} is the apparent wind speed. Both apparent wind speed and direction can be measured directly by the ultrasonic anemometer described in Section II.C.

The wind forces and moments can be expressed as:

$$\boldsymbol{\tau_w} = q \begin{bmatrix} C_X(\gamma_{rw})A_{Fw} \\ C_Y(\gamma_{rw})A_{Lw} \\ C_N(\gamma_{rw})A_{Lw}L_{aa} \end{bmatrix}, \tag{16}$$

Where A_{Fw} and A_{Lw} are the frontal and lateral projected windage areas (Fig. 5, Fig. 6). They are calculated precisely by the computer with projected 3D model. V_{rw} and γ_{rw} are apparent wind speed and angle of attack respectively, that can be measured directly from the anemometer introduced in section IIC.

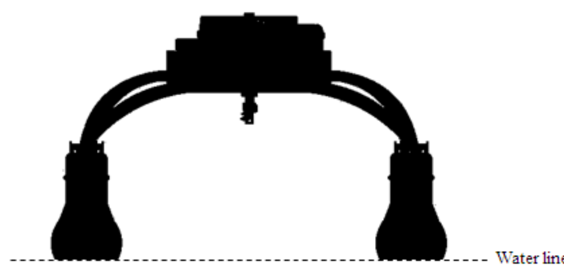

Fig. 5: Frontal projected area.

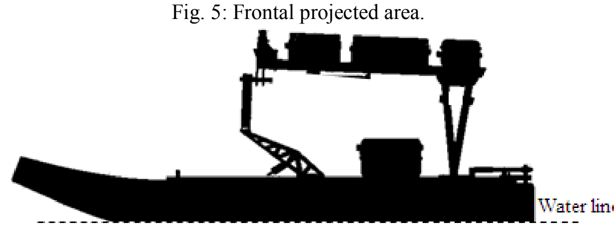

Fig. 6: Lateral projected area.

C_X, C_Y, C_Z are empirical wind coefficients in surge, sway and yaw direction respectively, and can be approximated by:

$C_X(\gamma_{rw}) = c_x cos(\gamma_{rw})$, $C_Y(\gamma_{rw}) = c_y sin(\gamma_{rw})$,

$C_Z(\gamma_{rw}) = c_z sin(2\gamma_{rw})$

In [25], it is suggested that $c_x \in \{-1.0, -0.8\}$, $c_y \in \{-1.0, -0.7\}$, and $c_z \in \{-0.2, -0.05\}$.

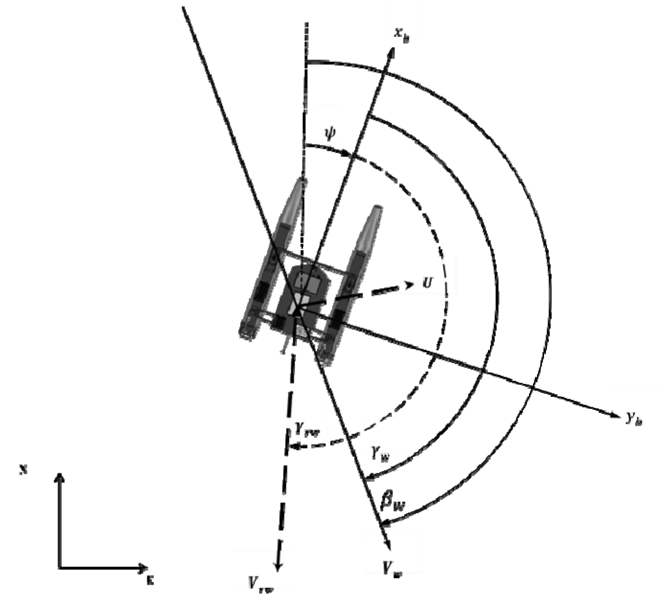

Fig. 7: Vehicle Heading (φ), Vehicle Velocity (U), True Wind Speed (V_w), True Wind Direction (β_w), True Wind Angle of Attack (γ_w), Apparent Wind Speed (V_{rw}), Apparent Wind Angle of Attack (γ_{rw})

c_x, c_y, c_z are picked to be $-0.7, -0.6, -0.1$ first in the model of wind feedforward controller. For the better performance of the feedforward controller, a coefficient matrix is introduced so that the wind feedforward control law was taken to be:

$$\boldsymbol{\tau_{ff}} = \mathrm{G_w}\boldsymbol{\tau_w}, \tag{17}$$

Where $\mathrm{G_w}$ is a 3×3 diagonal matrix, and

$$\mathrm{G_w} = diag(g_{w1}, g_{w2}, g_{w3}), \tag{18}$$

And here $0 \leq \mathrm{g_{wi}} \leq 1$ for i =1, 2, 3. $\mathrm{G_w}$ matrix is adaptive based on the reference model of the vehicle, and more detail about the adaptive tuning method of it will be discussed in section VC.

IV. System Identification

In order to get precise model of the WAM-V USV 16 for feedback sliding mode controller and wind feedforward design, a series sea trials, including bollard test, acceleration test, circle test, and zigzag test were conducted for the system identification. The azimuth angles of the thrusters δ_s and δ_p were kept at 0 degrees throughout the system characterization sea trials. The location was chosen to at the North Lake, Hollywood, FL that can provide a friendly environment with minimum wind, current and wave disturbances. Vehicle state was recorded throughout the experiments for calculation of model parameters and comparison with simulation results.

The main characteristics of the USV, such as overall length, draft, mass, etc., can be measured and were given in Table I. The added mass terms $X_{\dot{u}}$, $Y_{\dot{v}}$, $N_{\dot{r}}$ can be derived by semi-empirical equations as described in [25]. The terms that need to be identified are linear and nonlinear drag terms X_u, Y_v, N_r, and$X_{u|u|}$. Acceleration tests were conducted to get linear and nonlinear drag terms in surge direction X_u, and$X_{u|u|}$. Two types of circle tests carried out for Y_v , N_r. And zig-zag tests also performed for further validation of the identified model of USV.

A. Accleration Tests

The USV started from rest and accelerated with a set throttle on both motors for 60 seconds. A range of 70 -100 % of motor throttle commands were used to repeat the process for reliable experimental results. The relationship between motor commands and thrusts was estimated from a bollard test and can be seen in TABLE III

TABLE III
RELATIONSHIP OF MOTOR COMMAND AND THRUST FORM BOLLARD TEST

Motor Command [%]	50	60	70	80	90	100
Thrust [N]	190	203	215	228	241	254

Decouple surge movement from sway and yaw, the equation of motion is:

$$(m - X_{\dot{u}})\dot{u} + X_u + X_{u|u|}|u|N_r = T_x \tag{19}$$

When the vehicle achieved its steady speed $\dot{u} = 0$, the drag forces in surge direction are equal to the thrusts of the USV.

$$X_u + X_{u|u|}|u|N_r = T_x \tag{20}$$

By quadratic curve fitting of surge speeds and drag forces, X_u and $X_{u|u|}$ can be determined (Fig. 8).

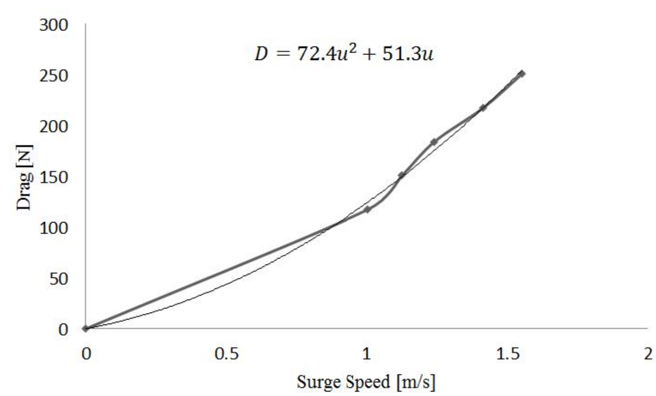

Fig. 8: Quadratic fit of surge speed and drag in surge direction for USV 16 model.

B. Circle Tests

Circle tests were conducted to get the drag term of N_r.

$$(I - \dot{N_r})\dot{r} + N_r r = M_z \tag{21}$$

During the circle test, the vehicle was first accelerated with 100% throttle on both sides for 20 seconds, then port and starboard were set to -100% and 100% throttle respectively for 30 seconds. Since the port and starboard propellers were both given full throttle, but with a phase difference of 180^0, the USV could make a tight turn around its center of gravity with no surge and sway velocity; the drag moment coefficient from yaw rate N_r could therefore be isolated.

When $\dot{r} \approx 0$, $N_r = M_z/r$. Similar to acceleration tests, repeated trials with a throttle of ±70, 80 90 % command were also carried out.

Another set of circle tests were also performed to derive the Y_v term. In this group of tests, port and starboard were set to 0% and 100% throttle instead of to -100% and 100%. Neglecting small quadratic velocity terms, the equation of motion in sway direction can be expressed as:

$$(m - Y_{\dot{v}})\dot{v} + (m - X_{\dot{u}})ur + Y_v v = T_y \quad (22)$$

In equation, the only unknown term is Y_v, so we can get the drag term in sway direction.

C. Zig-zag Tests

The zig-zag tests were utilized to evaluate the model. During the tests, the vehicle was first accelerated with 100% throttle on both sides for 20 seconds, then port and starboard were set to 100% and 0% throttle alternately four times on each side.

D. Simulation

Comparison of simulation and experimental results for the acceleration test, circle test and zig-zag test is shown in Fig. 9-Fig. 14.

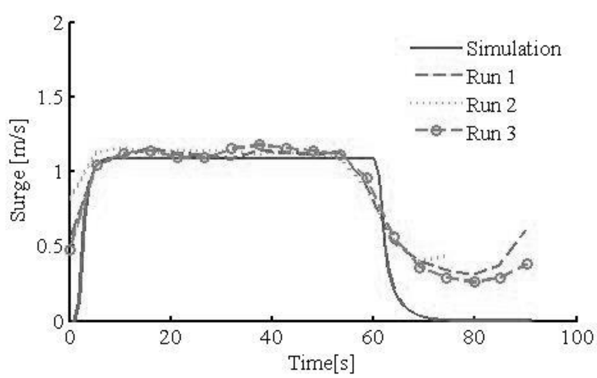

Fig. 9: Surge speed of simulation and experimental results of 70% throttle command during acceleration tests.

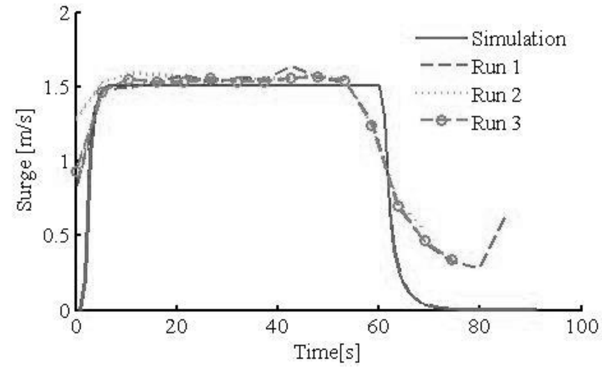

Fig. 10: Surge speed of simulation and experimental results of 100% throttle command during acceleration tests.

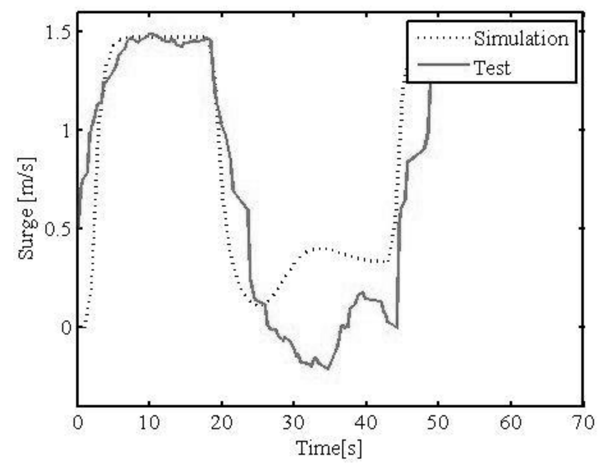

Figure 11: Surge speed of simulation and experimental results during circle tests.

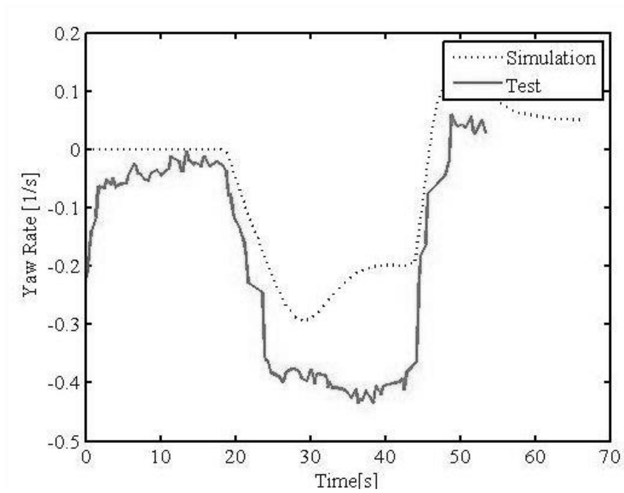

Fig. 12: Yaw speed of simulation and experimental results during circle tests.

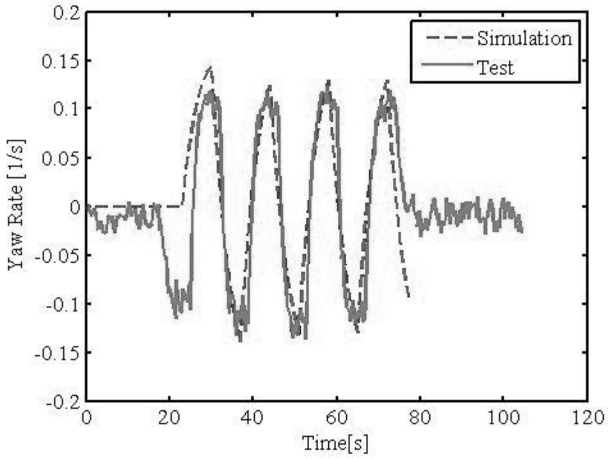

Fig. 13: Yaw rates of simulation and experimental results during zigzag tests with different throttle command (80% throttle).

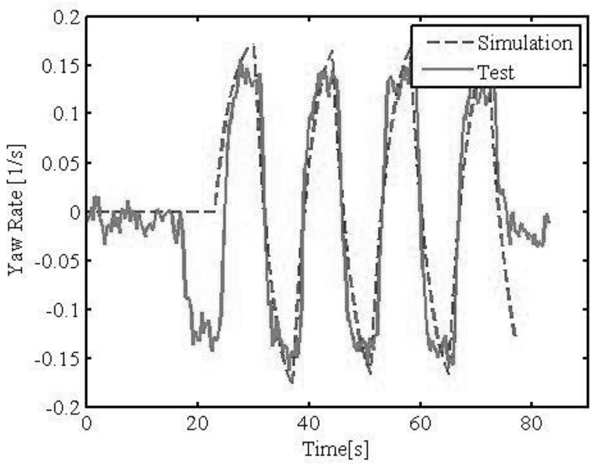

Fig. 14: Yaw rates of simulation and experimental results during zigzag tests with different throttle command (100% throttle).

V. CONTROLLER DESIGN

A. Nonlinear sliding mode feedback controller design

A robust sliding mode controller was designed on the USV for station keeping task. The sliding mode controller is a robust controller when dealing with modeling errors and uncertain parts of dynamics. The controller theory will be briefly introduced, and more details can be seen in [1].

First we define $\boldsymbol{\eta}_d = [x_d, y_d, \psi_d]^T$ to be the desired pose of the vehicle in the earth-fixed frame, then let $\boldsymbol{\eta}_t = \boldsymbol{\eta} - \boldsymbol{\eta}_d$ be the error vector, which is the difference between the desired pose and vehicle current pose.

A sliding surface function is defined as:

$$\boldsymbol{s} = \dot{\boldsymbol{\eta}}_t + 2\boldsymbol{\Lambda}\boldsymbol{\eta}_t + \boldsymbol{\Lambda}^2 \int_0^t \boldsymbol{\eta}_t dt. \qquad (23)$$

Here $\boldsymbol{\Lambda}$ represents the Lyapunov exponent gain vector and is designed based on various candidates frequencies.

Therefore, a newly defined reference trajectory is introduced:

$$\dot{\boldsymbol{\eta}}_r = \dot{\boldsymbol{\eta}}_d - 2\boldsymbol{\Lambda}\boldsymbol{\eta}_t - \boldsymbol{\Lambda}^2 \int_0^t \boldsymbol{\eta}_t dt. \qquad (24)$$

The sliding mode control law is defined as follows:

$$\boldsymbol{\tau} = \boldsymbol{M_1}\left(\boldsymbol{J}(\boldsymbol{\eta})^T \ddot{\boldsymbol{\eta}}_r + \boldsymbol{J}(\dot{\boldsymbol{\eta}})^T \dot{\boldsymbol{\eta}}_r\right) + \boldsymbol{C_1}(\boldsymbol{v})\boldsymbol{J}(\boldsymbol{\eta})^T \dot{\boldsymbol{\eta}}_r +$$

$$\boldsymbol{D_1}(\boldsymbol{v})\boldsymbol{J}(\boldsymbol{\eta})^T \dot{\boldsymbol{\eta}}_r - \boldsymbol{J}(\boldsymbol{\eta})^T \boldsymbol{R} * sat(\boldsymbol{E}^{-1} * \boldsymbol{s}) \qquad (26)$$

Where $\boldsymbol{R}$ represents the uncertainties, and $\boldsymbol{E}$ is the boundary layer thickness around the sliding surface $\boldsymbol{s}$.

An illustration of a linear signal for each element in $\boldsymbol{R}$ and $\boldsymbol{E}$ is given in a two-dimensional plot and can be seen in Fig. 15.

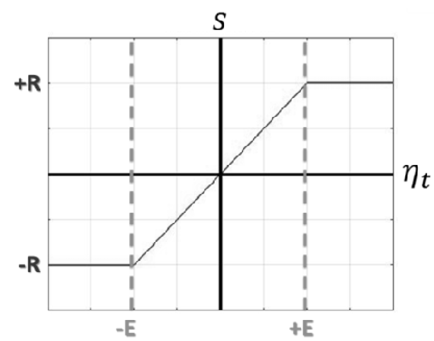

Fig. 15: Illustration of Saturation Function for a single saturation argument for Sliding Mode Controller

B. Wind feedforward controller design

Based on the mathematical model of vehicle's motion and wind forces and moments model discussed in section III, the wind load can $\boldsymbol{\tau_w} = \begin{bmatrix} T_{wx} \\ T_{wy} \\ M_{wz} \end{bmatrix}$ is calculated based on the wind model. The block diagram of the control system with wind feedforward controller is shown in Fig. 16.

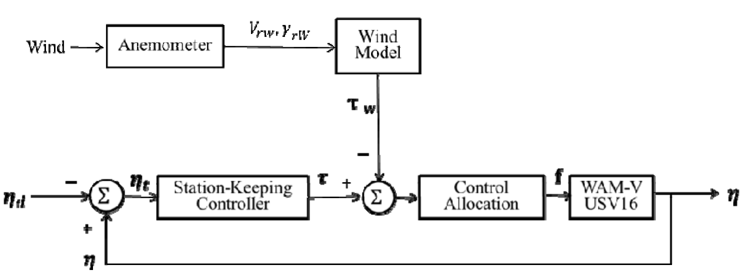

Fig. 16: Block Diagram of WAM-V USV 16 Control System with Wind Feedforward

The anemometer collected wind information, filtered the data, and then passed filtered apparent wind speed V_{rw} and direction γ_{rw} to the wind model as the input. The wind model calculated wind forces $\boldsymbol{\tau_w} = [T_{wx} \quad T_{wy} \quad M_{wz}]'$.

Therefore, to cancel out wind disturbance, we subtracted wind $\boldsymbol{\tau_w}$ from feedback control forces $\boldsymbol{\tau}$ to get the final control output $\boldsymbol{\tau_1} = \boldsymbol{\tau} - \boldsymbol{\tau_w}$. The control output will be fed into controller allocation block to get propeller thrust and azimuth angle. The control allocation method utilized here is a Lagrangrian multiplier approach, and can be found in [23].

C. Model reference adaptive feedforward controller design

In order to improve the performance of the wind feedforward controller during station keeping task, a model reference adaptive mechanism was developed.

The estimated wind loads in surge, sway and surge direction were multiplied by a feedforward gain matrix, as presented in [30].

The wind feedforward control law was taken to be:

$$\boldsymbol{\tau_{ff}} = \mathrm{G_w}\boldsymbol{\tau_w} \tag{27}$$

Where $\mathrm{G_w}$ is a 3×3 diagonal matrix,

$$\mathrm{G_w} = diag(g_{w1}, g_{w2}, g_{w3}) \tag{28}$$

And here $0 \le \mathrm{g_{wi}} \le 1$ for i =1, 2, 3.

VI. FIELD TESTS

Field tests were carried out in previous study of station keeping of the USV [16][31]. The location was chosen to be the calm water sections of the Intracoastal Waterway in Dania Beach, FL, USA, where sea states were less than 1, wind speeds less than 15 knots, wave heights less than 0.2 meters and without heavy currents. In this paper, the station keeping tasks were conducted at the North Lake, Hollywood, FL. Compared to the Intracoastal Waterway site, where the average wind speed was 1-2 m/s, the average wind speed (4-6 m/s) at the lake was much higher, and therefore the wind feedforward feature was more desirable.

The USV was initially brought to its desired position with desired heading using remote controller, and then switched to autonomous mode for 600 seconds. Thorough out the task, the vehicle position, heading, control efforts, wind speed and direction were recorded. The comparison of station keeping performances in respect to position error, heading error, control effort between nonlinear backstepping controller alone and feedback& adaptive feedforward controller were shown in Fig. 17- Fig. 20

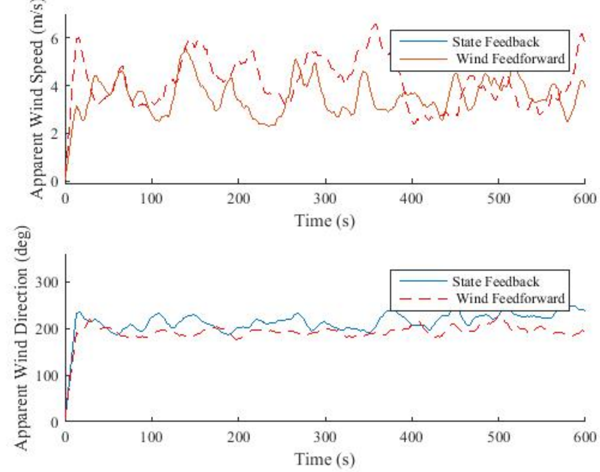

Fig. 17: Relative wind speed and direction during station keeping tasks without/ with wind feedforward control.

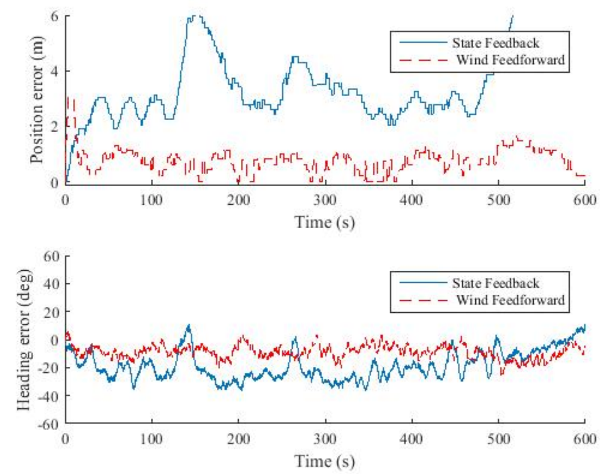

Fig. 18: Position and heading error during station keeping tasks without/ with wind feedforward control.

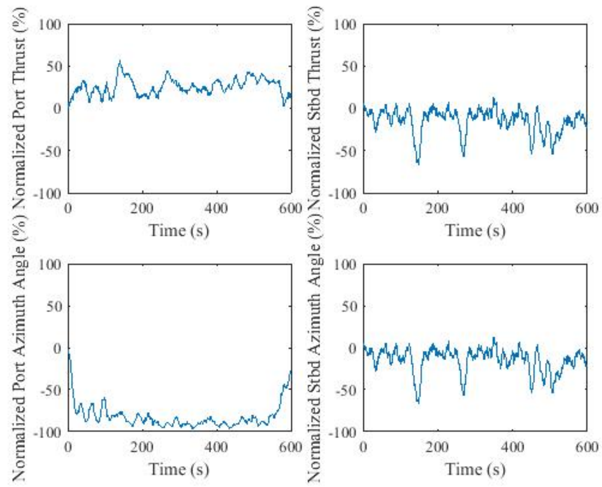

Fig. 19: Control effort (thrust and azimth angle of port and starboard in percentage) without wind feedforward control.

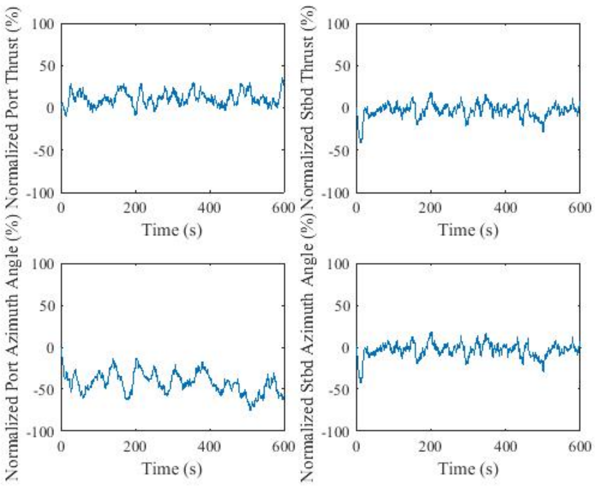

Fig. 20: Control effort (thrust and azimth angle of port and starboard in percentage) with wind feedforward control.

VII. CONCLUSIONS

In this paper, the station keeping controller of a USV was designed and tested. As a surface vehicle, the USV is light weight and susceptible to wind loads. Therefore, besides a nonlinear feedback sliding mode controller, a wind feedforward controller was also designed. An mechanism that adapts the gain matrix on the feedforward controller was developed for better control performance. Both feedback and feedforward controllers were built based on the vehicle's model formulated through system identification tests.

Experimental tests were conducted at North Lake, Hollywood, FL, where the average wind is about 5-6 m/s. The control performances in terms of position and heading errors as well as control efforts were compared. From Fig. 17 it can be seen that the relative wind speed and direction can be considered to be constant during station keeping tasks. Fig. 18 shows the position and heading errors over 600s for station keeping with and without feedforward control. The position error is the square root of the errors in the surge and sway directions; the heading error is the deviation from desired heading at the beginning of the test in the earth-fixed frame. Blue solid lines represent state feedback measurements using a single sliding mode controller, while the red dash line denotes control with both feedback and feedforward features. Without wind feedforward control, the USV can maintain its position and heading during a long period of time, even with strong environmental disturbances. However, when the adaptive feedforward controller is applied, the improvements in position and heading are significant (the position error is reduced from an average of 2.9 m to 0.8 m, and the heading error is reduced from -17.3^0 to -7.9^0). Finally Fig. 18 and Fig. 19 compare the control efforts for the two situations. From the plots it can be seen that with wind feedforward control, the amplitude of the commanded thrust is lower, but the station keeping performance is better.

REFERENCES

[1] Manley, J.E., Unmanned surface vehicles, 15 years of development, OCEANS 2008 , vol., no., pp.1,4, 15-18 Sept. 2008.

[2] Sarda, E., Dhanak, M. D., & von Ellenrieder, K. D., "Concept for a USV-based autonomous launch and recovery system" *ASNE Launch & Recovery 2014*, Linthicum, MD USA, 2014

[3] Karl-Petter W. Lindegaard. Acceleration Feedback in Dynamic Positioning.PhD thesis, Department of Engineering Cybernetics, Norwegian, University of Science and Technology, NO-7491 Trondheim, NORWAY, Sept 2003.

[4] IEEE Transactions of Control Systems Technology. Underactuated Dynamic Positioning of a Ship - Experimental Results, volume 8,September 2000.

[5] J. Ghommam, F. Mnif, A. Benali, and N. Derbel, "Asymptotic backstepping stabilization of an underactuated surface vehicle," IEEE Trans . on Control Systems Technology, vol. 14, no. 6, pp. 1150-1157, Nov. 2006.

[6] R. A. Soltan, H. Ashrafiuon, and K. R. Muske, "State-dependenttrajectory planning and tracking control of unmanned surface vehicles,"in Conf. 2009 American Control Conference , Hyatt Regency Riverfront ,2009,pp.3597-3602.

[7] Fossen, Thor I., and Jan P. Strand. "Tutorial on nonlinear backstepping: applications to ship control." *Modeling, identification and control* 20.2 (1999): 83-134.

[8] Sarda, E. I.; Qu, H.; Bertaska, I. R. & von Ellenrieder, K. D. (2015) "Development of a USV Station-Keeping Controller," *In MTS/IEEE Oceans-Genova, 2015 – Genova, May 2015* (pp. 1-10).

[9] Sarda, E., Lebbad, A., Anderson, J, Bertaska, I. Miranda II, M., Benson, M., Cheng, G., DeGaetano, D., Haizlett, K., Lapix, J., Long, A., Martinez, J., Mesa, B., Moscicki, T., Shu, E., Dr. Clayton, G., Dr. von Ellenrieder, K., & Dr. Nataraj, A. "Team WORX : Design and Development of an Autonomous USV for RobotX, The Inaugural Maritime Challenge, Singapore 2014", *Maritime RobotX Challenge 2014*, Singapore, Singapore, 2014

[10] Pereira, A.; Das, J.; Sukhatme, G., "An experimental study of station keeping on an underactuated ASV," Intelligent Robots and Systems, 2008. IROS 2008. IEEE/RSJ International Conference on , vol., no., pp.3164,3171, 22-26 Sept. 2008 doi: 10.1109/IROS.2008.4650991

[11] R. Stephens, "Wind feed-forward: blowing away the myths," in Dynamic Positioning Conference , October, 11-12,2011.

[12] Wind model MODELKitamura, F.; Sato, H.; Shimada, K.; Mikami, T., "Estimation of wind force acting on huge floating ocean structures," *OCEANS '97. MTS/IEEE Conference Proceedings* , vol.1, no., pp.197,202 vol.1, 6-9 Oct 1997

[13] Li Wenhua; Du Jialu; Sun Yuqing; Chen Haiquan; Zhang Yindong; Song Jian, "Modeling and simulation of marine environmental disturbances for dynamic positioned ship," *Control Conference (CCC), 2012 31st Chinese* , vol., no., pp.1938,1943, 25-27 July 2012

[14] Gould, R.W.F., 1982. The estimation of wind loads on ship superstructures.The Royal Institution of Naval Architects,monograph, 8, p.34.

[15] Isherwood, R.M., 1972. Wind resistance of merchant ships.Transportation Royal Institution of Naval Architects,1972(114), pp.327-338

[16]

[17]

[18] Hoday Stearns, Shuwen Yu, Sandipan Mishra, and Masayoshi Tomizuka. "Feedforward Tuning Methods for Wafer Scanning Systems."

[19] J.S. Vipperman, R.A. Burdisso, Adaptive feedforward control of non-minimum phase structural systems, Journal of Sound and Vibration, Volume 183, Issue 3, 8 June 1995, Pages 369-382, ISSN 0022-460X

[20] M.T. White, M. Tomizuka, Increased disturbance rejection in magnetic disk drives by acceleration feedforward control and parameter adaptation, Control Engineering Practice, Volume 5, Issue 6, June 1997, Pages 741-751, ISSN 0967-0661

[21] Wang, N.; Sun, J.-C.; Er, M.J.; Liu, Y.-C., "A Novel Extreme Learning Control Framework of Unmanned Surface Vehicles," Cybernetics, IEEE Transactions on , vol.PP, no.99, pp.1,1

[22] Klinger, W. B.; Bertaska, I. R.; Alvarez, José; von Ellenrieder, K. D., "Controller Design Challenges for Waterjet Propelled Unmanned Surface Vehicles with Uncertain Drag and Mass Properties." Proceedings of MTS/IEEE Oceans 2013 – San Diego. pp. 23-26. 2013.

[23] Bertaska, I. R., Alvarez, J., et.al., "Experimental Evaluation of Approach Behavior for Autonomous Surface Vehicles." In Proc. ASME Dynamic Systems Control Conference, 2013.

[24] Klinger, W. B., "Adaptive Controller Design for an Autonomous Twin-Hulled Surface Vessel with Uncertain Displacement and Drag, " Florida Atlantic University, Dania Beach, FL, USA, MS Thesis, 2014.

[25] T. I. Fossen, Guidance and Control of Ocean Vehicles. Chichester: John Wiley and Sons Ltd, 1994.

[26] Wind model MODELKitamura, F.; Sato, H.; Shimada, K.; Mikami, T., "Estimation of wind force acting on huge floating ocean structures," OCEANS '97. MTS/IEEE Conference Proceedings , vol.1, no., pp.197,202 vol.1, 6-9 Oct 1997

[27] Li Wenhua; Du Jialu; Sun Yuqing; Chen Haiquan; Zhang Yindong; Song Jian, "Modeling and simulation of marine environmental disturbances for dynamic positioned ship," Control Conference (CCC), 2012 31st Chinese , vol., no., pp.1938,1943, 25-27 July 2012

[28] Gould, R.W.F., 1982. The estimation of wind loads on ship superstructures.The Royal Institution of Naval Architects,monograph, 8, p.34.

[29] Isherwood, R.M., 1972. Wind resistance of merchant ships.Transportation Royal Institution of Naval Architects,1972(114), pp.327-338

[30] A.J. Sørensen, S.I. Sagatun, T.I. Fossen, Design of a dynamic positioning system using model-based control, Control Engineering Practice, Volume 4, Issue 3, March 1996, Pages 359-368, ISSN 0967-0661, http://dx.doi.org/10.1016/0967-0661(96)00013-5.

[31] Qu, H. Sarda, E. I. Bertaska, I. R. & von Ellenrieder, K. D. (2015) "Wind Feed-forward Control of a USV," *In MTS/IEEE Oceans-Genova, 2015 – Genova, May 2015* (pp. 1-10).